

In situ nucleation of carbon nanotubes by the injection of carbon atoms into metal particles

JULIO A. RODRÍGUEZ-MANZO¹, MAURICIO TERRONES¹, HUMBERTO TERRONES¹, HAROLD W. KROTO², LITAO SUN³ AND FLORIAN BANHART^{3*}

¹Advanced Materials Department, IPICYT, Camino a la Presa San José 2055, Col. Lomas 4a. sección, 78216 San Luis Potosí, México

²Department of Chemistry and Biochemistry, Florida State University, Tallahassee, Florida 32306-4390, USA

³Institut für Physikalische Chemie, Universität Mainz, 55099 Mainz, Germany

*e-mail: banhart@uni-mainz.de

Published online: 29 April 2007; doi:10.1038/nnano.2007.107

The synthesis of carbon nanotubes (CNTs) of desired chiralities and diameters is one of the most important challenges in nanotube science and achieving such selectivity may require a detailed understanding of their growth mechanism. We report the formation of CNTs in an entirely condensed phase process that allows us, for the first time, to monitor the nucleation of a nanotube on the spherical surface of a metal particle. When multiwalled CNTs containing metal particle cores are irradiated with an electron beam, carbon from graphitic shells surrounding the metal particles is ingested into the body of the particle and subsequently emerges as single-walled nanotubes (SWNTs) or multiwalled nanotubes (MWNTs) inside the host nanotubes. These observations, at atomic resolution in an electron microscope, show that there is direct bonding between the tubes and the metal surface from which the tubes sprout and can be readily explained by bulk diffusion of carbon through the body of catalytic particles, with no evidence of surface diffusion.

The effective application of nanotubes in electronic devices and highly advanced materials engineering will depend ultimately on our ability to specify the exact structure of individual nanotubes manufactured on a large scale—a goal that appears to be far from feasible at this time. There are several approaches to the production of CNTs and nanofibres¹. Chemical vapour deposition (CVD) is by far the most technically important method of production, and serious efforts have been made to determine the nanotube growth mechanism^{2–9}. In the majority of CVD approaches to the production of both SWNTs and MWNTs, catalytically active metal particles provide some degree of rough structural control. Several *in situ* electron microscopy CVD studies of carbon nanofibre growth in a gaseous hydrocarbon atmosphere have been reported^{2–4}. Evidence from these experiments indicates that the catalytic metal particles remain crystalline during the growth of carbon fibres, no intermediate metal-carbide phase is present before growth, and growth is initiated at steps on the catalytically active metal surface^{2,3}.

However, nucleation, as the first and most important step of nanotube growth, has never been accessible to observation and has remained unclear. Theoretical simulations of the initial stages of CNT growth have tended to disregard bulk carbon diffusion through the body of the catalyst because the energy barrier for such diffusion is higher than for migration on a metal surface or along a metal–graphene interface^{2,8}. The models differ from the earlier model proposed by Baker and others⁵ in which it was suggested that carbon dissolves into the metal particle at one place and diffuses through the bulk, and meso- or nanostructures

segregate at some other position. It is important to determine whether one or other of these two mechanisms occurs during nanotube nucleation and growth, or indeed whether both may occur, and under what conditions, because the production of nanotubes with precisely reproducible structure, which to date has not been achieved, will almost certainly depend on a deeper understanding of the nucleation and growth mechanisms. Such understanding could be key to the development of large-scale production of nanotubes with a desired structure and their eventual use in paradigm-shifting advances in electronic and civil engineering.

In the experiments described here, nanotubes have been created by the injection of carbon atoms into the body of catalytically active metal nanoparticles. The apparent successive segregation of the individual graphenic carbon networks from which the nanotube is ultimately composed is observed at the metal surface. This is a condensed-phase process in which no gaseous species are involved. The results were obtained by electron irradiation of MWNTs partly filled with transition metals. Previous studies have shown that electron irradiation of unfilled MWNTs can cause the collapse of the tubes and an injection of carbon atoms into the inner hollow cavities^{9–11}. In the present work, the irradiation of MWNTs containing encapsulated Co, Fe, FeCo, and Ni nanowires using a moderate strength electron beam resulted in the growth of SWNTs and MWNTs from the end faces of the metal particles inside the larger host tubes. This process was monitored with spatial resolution not achieved in previous real-time studies in which nanofibres have been created. Following

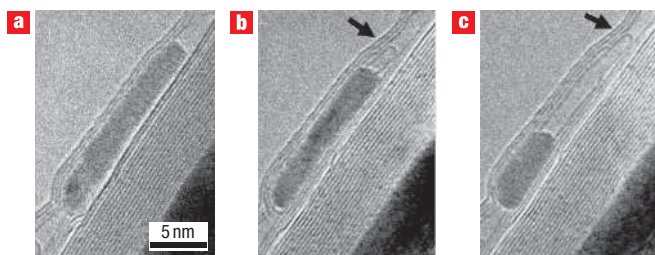


Figure 1 SWNT growth from a Co crystal. The series of images shows the growth of a single-walled CNT (arrowed) from a cobalt crystal inside a host nanotube. (The host nanotube is sitting on a larger Co-filled nanotube.) The growth happens under electron irradiation (intensity 100 A cm^{-2}) at a specimen temperature of $600 \text{ }^\circ\text{C}$. **a**, Image before growth. **b**, Image after 345 s of irradiation: a capped SWNT of $\sim 3 \text{ nm}$ in length has grown from the end face of the Co crystal. **c**, Image after 475 s; the SWNT has reached a length of 11 nm.

the previously reported *in situ* observation of carbon nanofibre growth^{2–4}, the present study is the first direct microscopic *in situ* observation of the nucleation and growth of CNTs.

RESULTS AND DISCUSSION

Multiwalled CNTs were filled with crystalline Fe, Co, FeCo or Ni nanowires^{12–14} (see Methods). Electron irradiation and imaging of the nanotubes was carried out in a transmission electron microscope (TEM) with an accelerating voltage of 300 kV. All TEM experiments were carried out at a specimen temperature of $600 \text{ }^\circ\text{C}$

using heating stages. Figure 1 shows the formation of a SWNT growing from a Co nanowire in the hollow core of a multiwalled tube during irradiation/observation under an electron-beam intensity of approximately 100 A cm^{-2} . In Fig. 1b a thin, capped SWNT is seen to grow from the encapsulated Co wire. The SWNT continues to grow as irradiation continues (Fig. 1c; see also Supplementary Information, Movie 1 to observe this growth process). According to lattice images and diffraction patterns, the metal crystals always remain solid and in the face-centred cubic (f.c.c.) phase throughout the process. No evidence for a regular crystalline cobalt carbide phase has been obtained. The Co crystal shrinks slightly owing to the diffusion of Co atoms through the carbon shells under irradiation¹⁵, but this phenomenon is unique here and does not obviously influence tube growth. The metal crystals often change their shape, but these transformations are slow and presumably due to diffusional creep under the pressure inside the nanotubes¹¹. In this study it should be noted that electron irradiation is essential for the growth of tubes; heating alone does not lead to an observable effect.

The growth of SWNTs was also observed inside MWNTs filled with Fe crystals, as shown in Fig. 2. Here the growth of the tube is accompanied by the appearance and migration of an oval domain inside the metallic core, which appears to exhibit a series of lattice fringes. Such domains were often observed in pure Fe crystals inside nanotubes, but not in FeCo or Co crystals. It is possible that this domain with a lattice spacing of 0.38 nm is carbidic (most likely Fe_3C , which has a 0.38-nm spacing of the 011 planes). The domain of this new phase appears to migrate from one end of the catalytic particle towards the opposite end, where new nanotube extrusion (growth) occurs (see arrows). The surrounding Fe crystal remains in the f.c.c. phase.

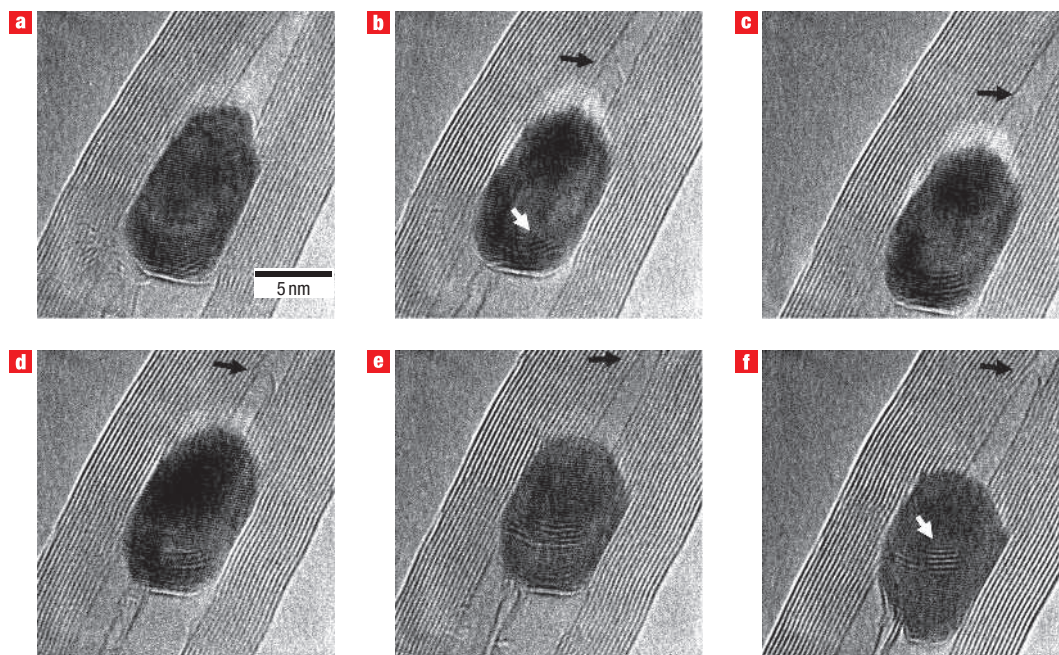


Figure 2 SWNT growth from Fe with possible occurrence of a carbide phase. The HRTEM images show the growth of a SWNT inside a MWNT, which is partly filled with a Fe crystal under electron irradiation ($\sim 200 \text{ A cm}^{-2}$ in intensity) at a specimen temperature of $600 \text{ }^\circ\text{C}$. The tip of the growing SWNT is indicated by a black arrow. **a**, Before nanotube growth, a cap with one carbon layer forms on the tip of the Fe particle, whose end face is becoming rounded. **b**, After 5 min of irradiation, a SWNT of 3.1 nm in length appears at the top of the particle and grows in the axial direction while the Fe crystal stays in place. A set of lattice fringes indicating the occurrence of a carbide phase appears on the bottom (white arrow). **c**, Image after 6 min, showing growth of the SWNT proceeding slowly. **d**, Image after 7 min. **e**, Image after 13 min. **f**, Image after 15 min, showing the tube growing and the carbide domain moving upwards.

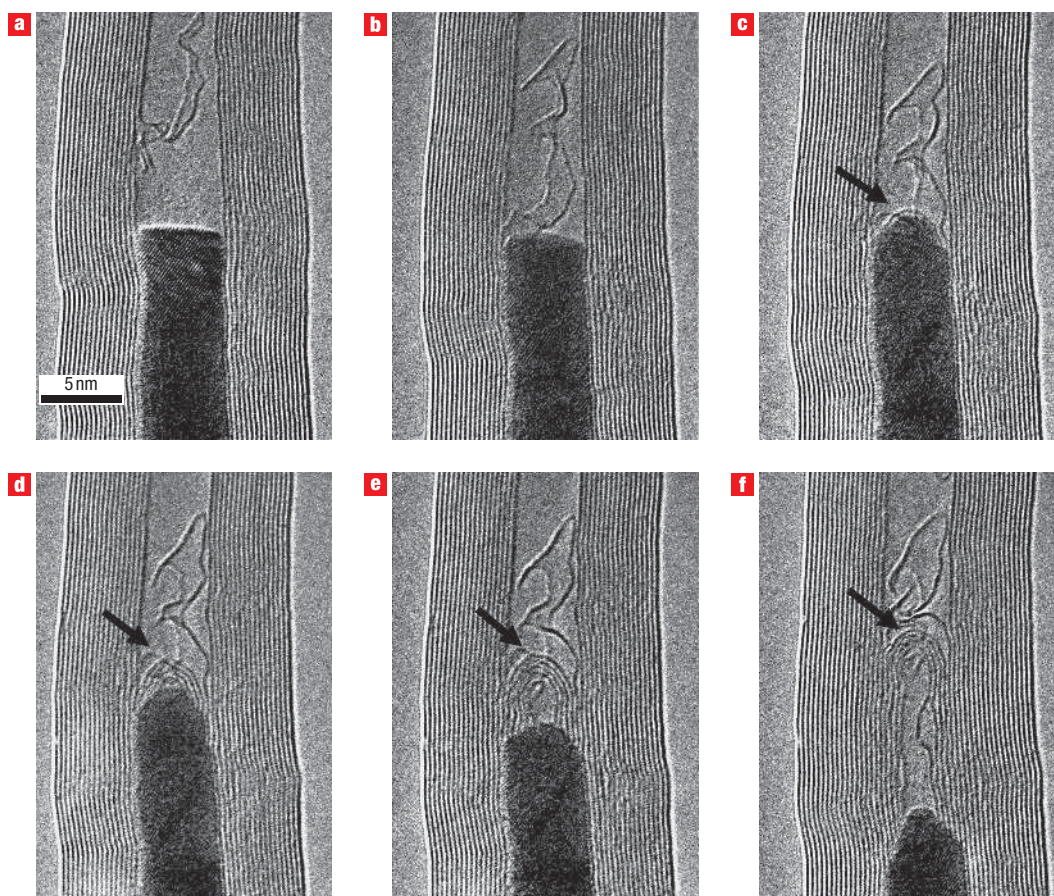


Figure 3 MWNT growth from a FeCo crystal. The image sequence shows the growth of a multiwalled CNT from a FeCo crystal inside a larger host nanotube under electron irradiation ($50\text{--}120\text{ A cm}^{-2}$) at a specimen temperature of $600\text{ }^{\circ}\text{C}$. The tip of the growing tube is arrowed. **a**, After a short period of irradiation, a graphitic sheet appears in the hollow core of the tube. The end face of the FeCo crystal is flat. **b**, After a further 360 s, the graphene sheet touches the crystal, whose end face starts becoming rounded. **c**, After 386 s, the graphene layer covers the round crystal face, and steps form where the ends of the graphene cap join the crystal. **d**, After 411 s, a new nanotube begins to grow, and the FeCo crystal slowly slides downwards. **e**, After 420 s, the MWNT has grown in length by approximately 5 nm. **f**, After 500 s, a five-layer MWNT is clearly visible.

The growth of a multiwalled tube from a FeCo (1:1 alloy) crystal is shown in Fig. 3. Initially, highly misshapen graphenic network filaments appear to aggregate in the central hollow core of the tube (Fig. 3a), which may be caused by the sputtering, under irradiation, of carbon from the inner wall into the hollow core¹⁰. A graphene sheet migrates inside the core and when it touches the FeCo crystal, it becomes attached to the surface (Fig. 3b). As soon as the metal tip surface is covered by the graphenic structure in the cavity above it, the metal tip, which was formerly flat, appears to deform into an almost hemispherical dome, and steps develop around the tip (Fig. 3c,d). Either simultaneously or shortly thereafter, the dome appears to be covered by a hemispherical graphenic cap (presumably a fullerenic half-cage), whose inner surface fits the dome essentially perfectly. The fact that the moment at which the graphenic ribbon appears to touch the metal surface and the moment when graphenic cap formation occurs are simultaneous suggests that the hemispherical shape of the metal tip is due to a wetting effect by the graphene surface layer.

As soon as the metal tip is round, nanotube growth starts because the first carbon layer segregating at the metal dome can form the cap of a tube. Almost immediately (Fig. 3d), three further graphenic caps form, one inside the other, with interlayer

separations close to the standard graphite distance, apparently materializing from the particle tip. The caps then become the tips of MWNTs, whose walls extrude from the particle, resulting in incipient formation of a new internal section of the original MWNT (see Supplementary Information, Movie 2, to observe this process). During growth, the metal inner core appears to slide in the opposite direction (downwards), perhaps owing to compressive forces inside the host tube¹¹. Although in this case migration of the metal particle accompanies nanotube growth, we have also observed growth where the metal core does not move (see Fig. 2). (See Supplementary Information, Fig. S1, for an example of MWNT formation involving a Co core.) It is important to note that all layers of the newly forming inner MWNT segments in Fig. 3 (see also Supplementary Information, Fig. S1) grow at exactly the same rate, that is, the inner layers grow at the same rate as the outer layers.

Figure 4 shows, with lattice resolution, the interface between a FeCo crystal and a CNT. On the upper side of the metal crystal (arrowed) it can be seen that the graphene layers of the tube are attached to the metal crystal by forming a strained quasi-coherent interface. The graphene layers are curved close to the interface so that they match the open lattice planes of the metal crystal. Owing to interfacial strain, the lattice of the metal

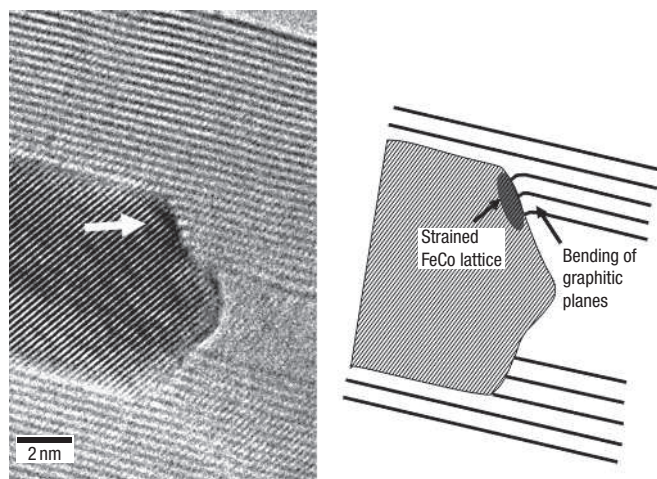


Figure 4 Interface between a FeCo crystal and a nanotube. Covalent bonds between the lattice planes of the metal and the nanotube lead to visible strain in both lattices; the graphitic layers are bent towards the metal, whereas the dark diffraction contrast in the metal close to the interface indicates a locally strained metal lattice. In the bottom half of the crystal this phenomenon does not appear, because the metal lattice planes to which the graphene layers are bonded are not in the appropriate projection to show lattice contrast in this specimen alignment. The drawing explains the important image details.

appears locally dark (this phenomenon of diffraction contrast is well known from TEM studies of strained-layer epitaxy). Thus, strong mechanical forces must act between the metal and the tube, which are readily explained by covalent metal–carbon bonds.

We have to consider three possible scenarios to explain the growth mechanism. The first is the bulk diffusion model, in which the only feasible source of carbon is the inner wall sections of the host nanotube, which are in direct contact with the metal particle. Presumably carbon atoms are knocked into the particle by the energetic electrons of the microscope beam¹⁰. The maximum energy transferred to a carbon atom by an electron of 300 keV energy is approximately 70 eV (ref. 16), which is high enough to cause carbon atom implantation into regions below the surface of the metal particles. A direct influence of electron irradiation on the structure or properties of the metals can be excluded because the displacement threshold energy in the metals is higher than the electron energy (300 keV) of these experiments, and electronic excitations are quenched by the presence of conduction electrons¹⁶.

The solubility of carbon in pure Fe or Co is low (carbon/metal atom ratio of less than $\sim 10^{-3}$) at the temperatures of this experiment, so a continuous migration of carbon atoms in low concentration through the metal appears to take place. Carbon atom diffusion in Co is fast, with a diffusion coefficient of $1.4 \times 10^{-14} \text{ m}^2 \text{ s}^{-1}$ at 600 °C (ref. 17). Because of their low solubility in the metal, the injected carbon atoms leave the metal and segregate at the uncovered surface as extended arrays of ordered hexagonal carbon networks. We have calculated the number of carbon atoms that are displaced from the host tubes into the metal particles by taking into account the displacement dynamics¹⁶, the solubility and diffusivity of carbon in the metal, and the geometry of the system (for details of the calculation, see Supplementary Information). For the case shown in Fig. 1, we obtained a growth speed of approximately 1 nm min^{-1} of the SWNT. This result is in good agreement with the observed growth speed of 1.4 nm min^{-1} in Fig. 1.

The second possible mechanism is the surface diffusion model. If we assume the supply of carbon atoms by diffusion on the metal surface¹⁸, atoms that are sputtered from the shells of the host tube would have to migrate along the interface between the metal and the host tube until they reach the curved end of the metal cylinder. Here the nucleation and growth of a single shell could happen, but it is difficult to see how such a process could explain the clear evidence obtained in this study that several concentric nanotubes sprout simultaneously and grow at the same rate from the carbon particle. As the supply of carbon atoms comes from outside, the atoms would have to penetrate the outer shells of the growing tube to reach the inner shells. In the example shown in Fig. 3, the atoms would have to jump through four layers without leading to nanotube growth in any of them until they reach the inner layer. The barrier for the migration of carbon atoms through graphene shells by site exchange is 2.3 eV (ref. 19) (the energy barrier for penetration through closed hexagons without atom exchange would be 10 eV, which is prohibitively high). Because of the clear direct contact between the growing graphene cylinders and the metal crystal, as seen in Fig. 4, there would always be a rather large energy barrier preventing any tunnelling of carbon atoms towards the inner shells.

If we assume that the penetration of carbon atoms through nanotube shells is possible and occurs at a high rate, this process would already happen when carbon atoms migrate along the interface between the metal and the host tube. Because the supply of carbon atoms in the surface diffusion model is non-uniform (more atoms arrive at the outer than at the inner shells of the growing tube), the only possibility to explain the observed uniform growth of a MWNT would be a rate-limiting chemical process at the metal–tube interface. However, because we observe growth speeds of only 1 nm min^{-1} , and this is orders of magnitude lower than in CVD experiments, a rate-limiting interfacial reaction is not a plausible explanation. Hence, surface diffusion of carbon atoms along the metal–tube interface is certainly possible, but one would expect such a mechanism to result in preferential growth of the outermost layers of the new MWNT sections. This would also be expected if the carbon atoms originate from the empty core of the host tube, because the atoms could only reach the metal surface by diffusing between the host tube and the outermost layer of the new tube.

The third possibility is the carbide model. Before irradiation, the metal particles do not contain significant amounts of carbides. During irradiation, some carbide domains might form in Fe crystals (see Fig. 2), but not in Co, as no indications of cobalt carbide are observed. In Fe, such a process is not unexpected, as a similar phenomenon has been observed to occur when carbon onions containing encapsulated Fe crystals are exposed to electron irradiation²⁰. The carbidic domains (Fig. 2) appear to migrate through the Fe crystals towards the end face from which CNT growth is observed. At the end face of the metal, decomposition of the carbide may lead to the precipitation of carbon and eventually growth of a tube. Such a scenario has been suggested by Schaper *et al.*⁹ who observed the segregation of carbon at the end face of carbide crystals inside nanotubes.

The dynamics of the morphological changes that occur, as witnessed in the various individual examples recorded here, indicates very strongly that carbon atoms diffuse at least in part in some way through the metal particle. We suggest the following highly plausible growth scenario for the formation of SWNTs and MWNTs catalysed by metal particles (Fig. 5). (1) Carbon atoms from the host MWNT are knocked into the metal particle by the electron beam (occasionally also into the empty hollow core). (2) The more-or-less flat end of the metal particle appears to deform forming a convex dome, and this seems to be a necessary condition for the nucleation of a nanotube.

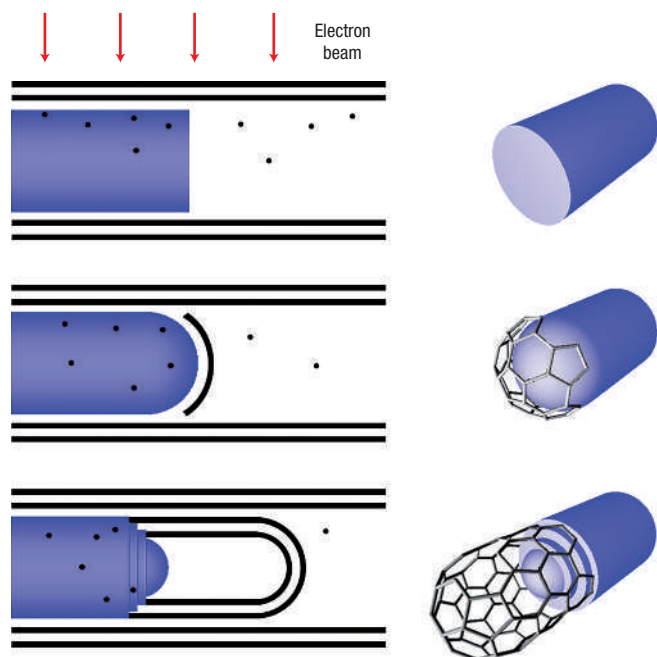


Figure 5 Mechanism of nanotube growth. **a**, Carbon atoms are displaced by the electron beam into the metal crystal and the hollow core of the host nanotube. **b**, When the end face of the metal becomes rounded, a hemispherical graphene cap forms and serves as the starting point for nanotube growth. **c**, A new nanotube grows from steps on the metal surface. Carbon atoms are fed from the metal crystal.

(3) Apparently simultaneously, a surface-covering carbon cap appears, which almost certainly is a hemispherical fullerene structure. The forces causing the dome formation may be wetting effects. (4) Around the edge, at the base of the dome, steps develop from where the walls of new MWNT segments sprout. The shape of the hemispherical dome defines the curvature of the new nanotube cap. (5) Carbon atoms are fed continuously into the metal particle, through which they diffuse rapidly to supply the root regions of the growing MWNTs. Transport of carbon atoms through the regions of the immediate subsurface layers of the metal particle^{18,21} might also explain our observations in part but again would be expected to favour growth of the outer layers of the new MWNTs, because these would be the first nucleation sites that the carbon atoms reach.

To conclude, it has been shown by electron microscopy that metal-filled MWNTs can act as convenient reaction cells in which the microscope's electron beam can induce metal-catalysed SWNT and MWNT growth and simultaneously monitor the *in situ* nucleation and growth process at very high resolution. The observations indicate that the CNT growth mechanism is essentially the same whether the catalyst is Fe, Co, Ni or an Fe/Co alloy. The most compelling explanation of the results is that the carbon atoms, which serve as feedstock for further nanotube growth, appear to be ingested directly into the crystalline catalytic metallic cores from the graphitic walls of the original MWNT during electron irradiation followed by migration through the metal to the hemispherical surface regions from which the new nanotubes sprout. It is also demonstrated that the growing tube is attached firmly to the metal crystal by covalent bonds. Although this new nanotube formation process differs from the CVD technique commonly used for nanotube production, the fact that very similar structures result

suggests that some of the detailed insights into the growth mechanism that the present experiments yield also apply to the CVD process. The ingestion mechanism for supplying the carbon atoms necessary for generating CNTs may also provide a new avenue for the investigation of large-scale nanotube fabrication.

METHODS

MWNT-encapsulated metal nanowires were produced in a CVD reaction chamber by the pyrolysis of the vapour derived from a hydrocarbon–organometallic solution^{12–14}. For Fe-filled, Co-filled, Ni-filled and FeCo alloy-filled MWNTs, solutions of ferrocene dissolved in ethanol, Co acetylacetonate dissolved in toluene, Ni acetylacetonate dissolved in toluene, or a mixture of ferrocene and cobaltocene dissolved in toluene were used, respectively¹⁴. All the solutions were 3 wt% organometallic compound(s) to their respective solvent. The solutions were then atomized in the presence of Ar, and the resulting aerosol directed into a quartz tube furnace operating at different temperatures depending on the catalyst: 950 °C for ferrocene, 850 °C for Co, 900 °C for Ni and 650 °C for the FeCo alloy. The resulting MWNT material was scraped from the tube walls. The powders consisting of partially filled MWNTs were dispersed ultrasonically in ethanol and deposited on a copper grid to enable *in situ* electron microscopy experiments to be carried out. TEM experiments were carried out with an FEI Tecnai F-30 located at the University of Mainz.

Received 22 December 2006; accepted 27 March 2007; published 29 April 2007.

References

- Dai, H. Nanotube growth and characterization in *Carbon Nanotubes: Synthesis, Structure and Applications* (eds Dresselhaus, M. S., Dresselhaus, G. & Avouris, P.) 29–53 (Springer, Berlin/Heidelberg, 2001).
- Helveg, S. *et al.* Atomic-scale imaging of carbon nanofiber growth. *Nature* **427**, 426–429 (2004).
- Lin, M. *et al.* Direct observation of single-walled carbon nanotube growth at the atomic scale. *Nano Lett.* **6**, 449–452 (2006).
- Sharma, R. & Iqbal, Z. In situ observations of carbon nanotube formation using environmental transmission electron microscopy. *Appl. Phys. Lett.* **84**, 990–992 (2004).
- Baker, R. T. K., Harris, P. S., Thomas, R. B. & Waite, R. J. Formation of filamentous carbon from iron, cobalt and chromium catalyzed decomposition of acetylene. *J. Catal.* **30**, 86–95 (1973).
- Raty, J. Y., Gygi, F. & Galli, G. Growth of carbon nanotubes on metal nanoparticles: a microscopic mechanism from ab-initio molecular dynamics simulations. *Phys. Rev. Lett.* **95**, 096103 (2005).
- Gavillet, J. *et al.* Root-growth mechanism for single-wall carbon nanotubes. *Phys. Rev. Lett.* **87**, 275504 (2001).
- Hofmann, S., Csanyi, G., Ferrari, A. C., Payne, M. C. & Robertson, J. Surface diffusion: the low activation energy path for nanotube growth. *Phys. Rev. Lett.* **95**, 036101 (2005).
- Schaper, A. K., Hou, H. Q., Greiner, A. & Philipp, F. The role of iron carbide in multiwalled carbon nanotube growth. *J. Catal.* **222**, 250–254 (2004).
- Banhart, F., Li, J. X. & Krasheninnikov, A. V. Carbon nanotubes under electron irradiation: stability of the tubes and their action as pipes for atom transport. *Phys. Rev. B* **71**, 241408 (2005).
- Sun, L. *et al.* Carbon nanotubes as high pressure cylinders and nanoextruders. *Science* **312**, 1199–1202 (2006).
- Kamalakaran, R. *et al.* Synthesis of thick and crystalline nanotube arrays by spray pyrolysis. *Appl. Phys. Lett.* **77**, 3385–3387 (2000).
- Mayne, M. *et al.* Pyrolytic production of aligned carbon nanotubes from homogeneously dispersed benzene-based aerosols. *Chem. Phys. Lett.* **338**, 101–107 (2001).
- Elias, A. L. *et al.* Production and characterization of single-crystal FeCo nanowires inside carbon nanotubes. *Nano Lett.* **5**, 467–472 (2005).
- Banhart, F., Redlich, Ph. & Ajayan, P. M. The migration of metal atoms through carbon onions. *Chem. Phys. Lett.* **292**, 554–560 (1998).
- Banhart, F. Irradiation effects in carbon nanostructures. *Rep. Prog. Phys.* **62**, 1181–1221 (1999).
- McLellan, R. B., Ko, C. & Wasz, M. L. The diffusion of carbon in solid cobalt. *J. Phys. Chem. Solids* **53**, 1269–1273 (1992).
- Abild-Pedersen, F., Nørskov, J. K., Rostrup-Nielsen, J. R., Sehested, J. & Helveg, S. Mechanisms for catalytic carbon nanofiber growth studied by ab-initio density functional theory calculations. *Phys. Rev. B* **73**, 115419 (2006).
- Xu, C. H., Fu, C. L. & Pedraza, D. F. Simulations of point defect properties in graphite by a tight-binding force model. *Phys. Rev. B* **48**, 13273–13279 (1993).
- Sun, L. & Banhart, F. Graphitic onions as reaction cells on the nanoscale. *Appl. Phys. Lett.* **88**, 193121 (2006).
- Amara, H., Bichara, C. & Ducastelle, F. Formation of carbon nanostructures on nickel surfaces: a tight-binding grand canonical Monte Carlo study. *Phys. Rev. B* **73**, 113404 (2006).

Acknowledgements

Support from the Deutsche Forschungsgemeinschaft (BA 1884/4-1) and the International Max Planck Research School in Mainz (J.A.R.-M.) is gratefully acknowledged. We also thank CONACYT-Mexico for scholarship (J.A.R.-M.) and grants 45772 (M.T.), 45762 (H.T.), 42428-Inter American Collaboration (H.T.), 41464-Inter American Collaboration (M.T.), 2004-01-013-SALUD-CONACYT (M.T.) and PUE-2004-CO2-9 Fondo Mixto de Puebla (M.T.). We thank A. Elias and A. Zamudio for assistance in the preparation of the FeCo sample and A. Krasheninnikov for fruitful discussions. H.W.K. thanks The Florida State University for financial support.

Competing financial interests

The authors declare that they have no competing financial interests.

Reprints and permission information is available online at <http://npg.nature.com/reprintsandpermissions/>